Performance Analysis of High-temperature Chemical Heat Pump with Metal Hydrides

Yunting Ge, Xinyu Zhang, Arton Merovci
School of the Built Environment and Architecture, London South Bank University
103 Borough Road, London ,SE1 0AA, UK
yunting.ge@lsbu.ac.uk

Engineering and Physical Sciences Research Council

London South Bank University

Innovate UK

Waste heat recovery from industrial sites (~35°C & ~230°C) with advanced heat pump technology to obtain heat (~130°C)

- In an energy-intensive industrial site such as a steel plant, there is plenty of medium and low-temperature waste heat which could be recovered for heating purposes with advanced metal hydride (MH) heat pumps.
- Compared to other heat pump systems the MH heat pump has some distinct advantages including low electrical power input, environmentally friendly working medium, compactness, and high-temperature heat delivery.
- Key challenges, however, are identification of suitable alloys and their characterisation for high-temperature MH heat pump application. This needs to be done before any theoretical and experimental analyses can be performed.
- To address these, a test rig for the high temperature MH heat pump research has been designed and fabricated. Correlation models for MH alloy selections and initial characterisation of MH alloys have been developed followed by the development of a transient heat pump simulation model.

Engineering and Physical Sciences Research Council
London South Bank University EST 1892
Innovate UK

Comparison between metal hydride and absorption heat pump cycles

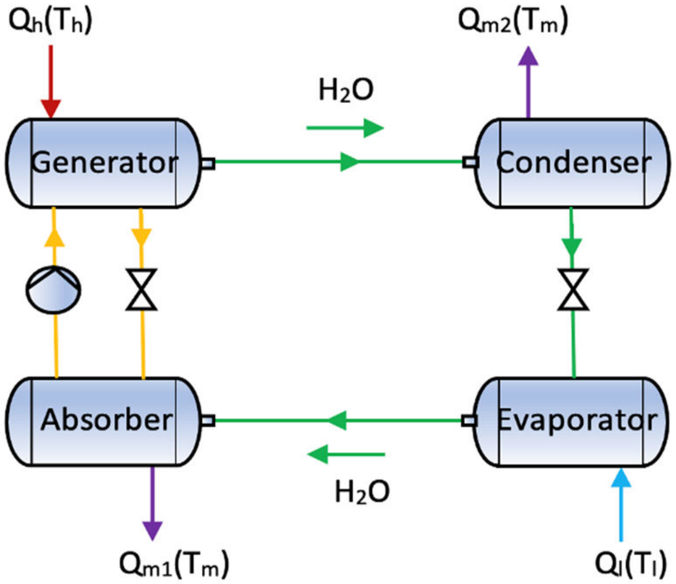

Absorption Heat Pump Cycle

Comparison of Two Heat Pump Cycles

Heat Pump Cycle	Working fluid	Absorbent	Energy input	COP	Dimension	Heat output temperature range
Absorption	H2O/NH3	LiBr/H2O	Thermal	1.2~1.3	Large	Limited
Metal Hydride	H2	Metal Hydride Alloy such as $LaNi_5$ or TiFe etc	Thermal	1.2~1.3	Small	Large

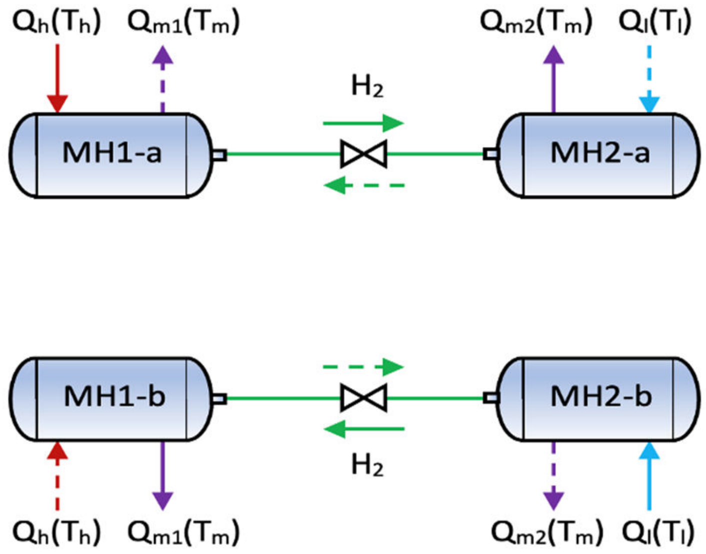

Metal Hydride (MH) Heat Pump Cycle

UKRI Engineering and Physical Sciences Research Council

London South Bank University

UKRI Innovate UK

Selection of metal hydride alloys

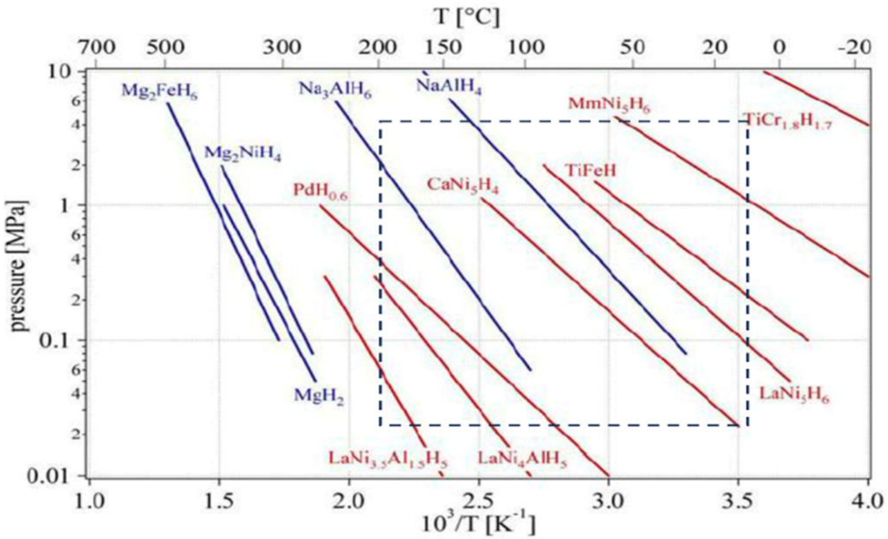

Operating temperature and pressure range of different alloys

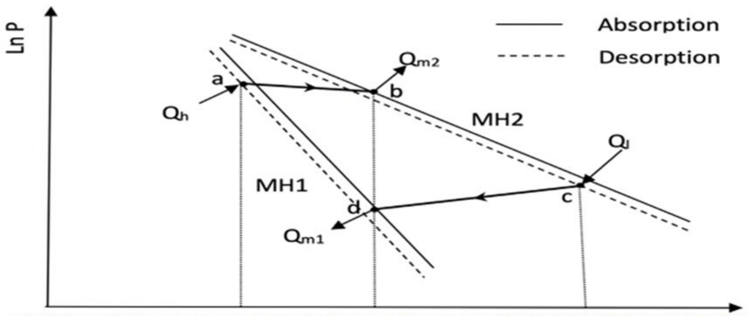

For each reaction process, the van't Hoff's law applies with following form:

$$\ln P_{H_2} = -\frac{\Delta H \times 1000}{RT} + \frac{\Delta S}{R}$$

To facilitate the MH alloy selection, P_h and P_l are assumed the same as P_{m2} and P_{m1} correspondingly. In that case, the following formulas will follow:

$$-\frac{\Delta H_1 \times 1000}{T_h} + \Delta S_1 = -\frac{\Delta H_2 \times 1000}{T_m} + \Delta S_2$$

$$-\frac{\Delta H_1 \times 1000}{T_m} + \Delta S_1 = -\frac{\Delta H_2 \times 1000}{T_l} + \Delta S_2$$

$$\eta = \frac{\Delta S_1 - \Delta S_2}{\Delta H_2} \qquad \xi = \frac{\Delta H_1}{\Delta H_2}$$

$$\eta = \left(\frac{\xi}{T_h} - \frac{1}{T_m}\right) \times 1000$$

$$\eta = \left(\frac{\xi}{T_m} - \frac{1}{T_l}\right) \times 1000$$

Engineering and Physical Sciences Research Council

London South Bank University

EST 1892

Innovate UK

MH alloys to be selected-thermodynamic analysis

$$\eta = \left(\frac{\xi}{T_h} - \frac{1}{T_m}\right)\times 1000$$

$$\eta = \left(\frac{\xi}{T_m} - \frac{1}{T_l}\right)\times 1000$$

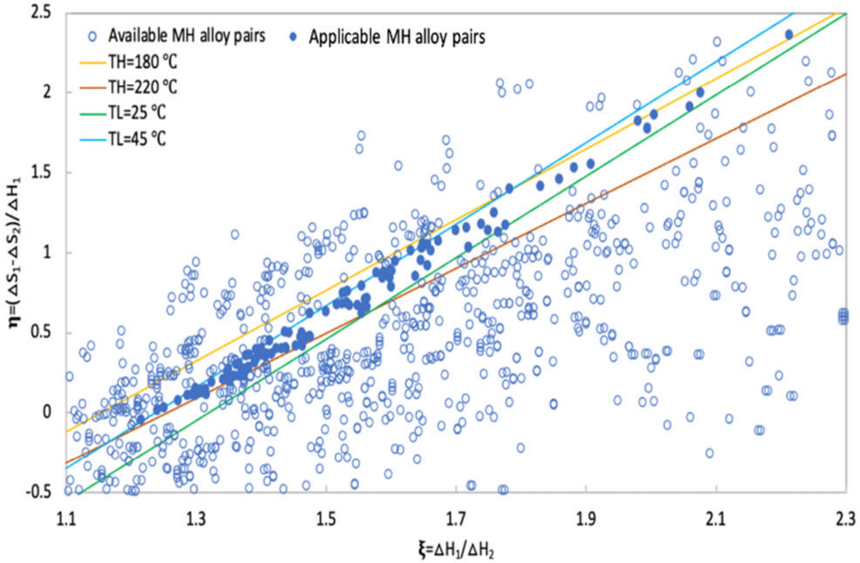

Coordinate points (**ξ** , **η**) for the applicable MH alloys and four straight lines at maximum and minimum temperatures of T_h and T_l, and constant temperature T_m**(=120°C)**

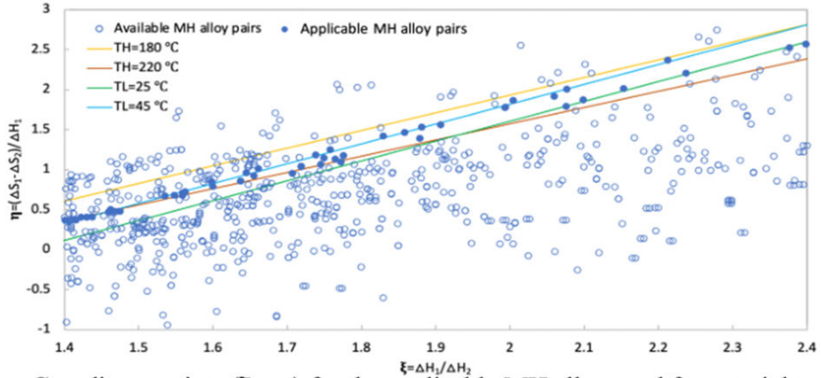

Coordinate points (**ξ** , **η**) for the applicable MH alloys and four straight lines at maximum and minimum temperatures of T_h and T_l, and constant temperature T_m**(=130°C)**

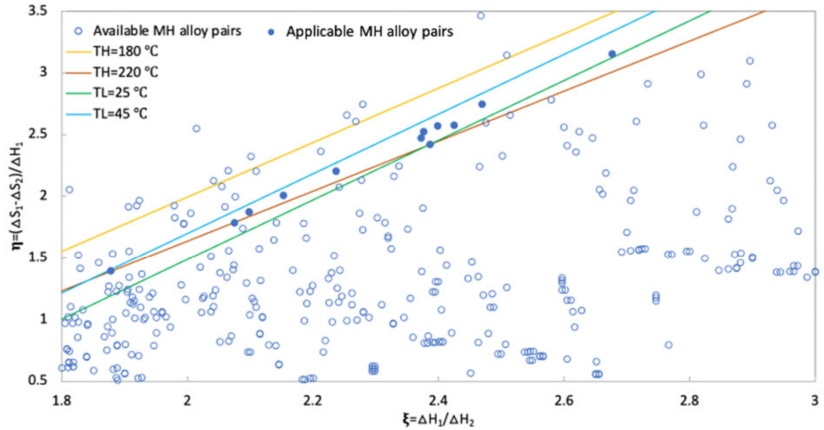

Coordinate points (**ξ** , **η**) for the applicable MH alloys and four straight lines at maximum and minimum temperatures of T_h and T_l, and constant temperature T_m**(=140°C)**

Engineering and Physical Sciences Research Council

London South Bank University

Innovate UK

Identification of applicable MH alloy pair for the MHHP system

Applicable MH alloy pairs for T_m=130 ℃

Pair No	MH alloy pair		COA	COAc	ψ	W_1	W_2	P_h	P_l	T_h	T_l
	HT MH alloy	LT MH alloy				kg	kg	bar	bar	°C	°C
1	$LaNi_{4.6}Al_{0.4}$	$CeNi_3Cu_2$	0.946	1.421	0.666	0.59	1	51.122	9.853	202.04	23.20
2	$LaNi_{4.5}Al_{0.5}$	$Ce_{1.1}Ni_{2.5}Cu_{2.5}$	0.995	1.538	0.647	0.395	1	35.947	6.789	198.44	44.36
3	$LaNi_{4.6}Al_{0.4}$	$CeNi_{2.5}Cu_{2.5}$	1.003	1.464	0.685	0.589	1	56.178	9.853	206.95	26.55
4	$CaNi_5$	$CeNi_3Cu_2$	1.032	1.482	0.697	0.525	1	51.122	14.823	190.51	44.05
5	$LaNi_{4.7}Al_{0.3}$	$CeNi_{2.5}Cu_{2.5}$	1.093	1.499	0.729	0.441	1	56.178	15.518	188.77	48.06
6	$LaNi_{4.25}Al_{0.75}$	$Zr_{0.9}Ti_{0.1}Cr_{0.6}Fe_{1.4}$	1.251	1.532	0.816	2.06	1	25.079	2.646	212.56	32.42
7	$LaNi_{4.30}Mn_{0.70}$	$ZrCr_{0.6}Fe_{1.4}$	1.286	1.608	0.800	0.714	1	15.660	1.926	206.03	46.54
8	$LaNi_{4.75}Al_{0.25}$	$Ti_{0.98}Zr_{0.02}V_{0.41}Fe_{0.09}Cr_{0.05}Mn_{1.46}$	1.299	1.572	0.827	2.13	1	105.369	18.880	210.21	39.29
9	$LaNi_{4.5}Al_{0.5}$	$Zr_{0.8}Ti_{0.2}Cr_{0.6}Fe_{1.4}$	1.301	1.699	0.766	0.93	1	58.536	6.789	223.09	44.69
10	$LaNi_{4.7}Al_{0.3}$	$Ti_{0.98}Zr_{0.02}V_{0.41}Fe_{0.09}Cr_{0.05}Mn_{1.46}$	1.321	1.586	0.833	1.38	1	105.369	15.518	224.22	31.47
11	$LaNi_{4.5}Al_{0.5}$	$La_{0.6}Y_{0.4}Ni_{4.8}Mn_{0.2}$	1.329	1.703	0.781	0.867	1	56.311	6.789	221.04	46.27
12	$LaNi_{4.56}Mn_{0.44}$	$La_{0.6}Y_{0.4}Ni_{4.8}Mn_{0.2}$	1.330	1.685	0.789	0.698	1	56.311	6.342	221.70	44.15
13	$LaNi_{4.8}Al_{0.2}$	$Ti_{0.98}Zr_{0.02}V_{0.41}Fe_{0.09}Cr_{0.05}Mn_{1.46}$	1.348	1.569	0.859	1.25	1	105.369	23.342	198.23	48.21
14	$LaNi_{4.83}Mn_{0.17}$	$CeNi_4Zr$	1.439	1.611	0.893	3.85	1	140.580	22.112	218.26	38.39
15	$LaNi_{4.8}Al_{0.2}$	$CeNi_4Zr$	1.464	1.604	0.913	2.87	1	140.580	23.342	214.01	40.47
16	$LaNi_{4.81}Mn_{0.28}Al_{0.15}$	$La_{0.6}Y_{0.4}Ni_{4.8}Mn_{0.2}$	1.375	1.714	0.802	0.52	1	56.311	7.232	219.40	48.26
17	$LaNi_{4.81}Mn_{0.28}Al_{0.15}$	$Zr_{0.8}Ti_{0.2}Cr_{0.6}Fe_{1.4}$	1.346	1.710	0.787	0.56	1	58.536	7.232	221.47	46.68
18	$LaNi_{4.83}Mn_{0.17}$	$Ti_{0.98}Zr_{0.02}V_{0.41}Fe_{0.09}Cr_{0.05}Mn_{1.46}$	1.330	1.575	0.844	1.68	1	105.369	22.112	202.04	45.89
19	$LaNi_{4.8}Al_{0.2}$	$CeNi_4Cr$	1.326	1.477	0.898	2.50	1	129.697	23.342	209.49	26.44
20	$LaNi_{4.8}Al_{0.2}$	$Ti_{0.99}Zr_{0.01}V_{0.43}Fe_{0.09}Cr_{0.05}Mn_{1.6}$	1.312	1.567	0.838	1.22	1	145.585	23.342	215.99	34.53
21	$LaNi_{4.56}Mn_{0.44}$	$Zr_{0.8}Ti_{0.2}Cr_{0.6}Fe_{1.4}$	1.301	1.681	0.774	0.748	1	58.536	6.342	223.71	42.58
22	$LaNi_4Al$	$La_{0.6}Y_{0.4}Ni_{4.8}Al_{0.2}$	1.295	1.563	0.829	3.7	1	14.921	1.521	221.31	46.60
23	$LaNi_{4.8}Al_{0.2}$	$CeNi_3Cr_2$	1.272	1.417	0.898	2.713	1	125.899	30.032	207.85	35.55
24	$LaNi_4Al$	$ZrCr_{0.6}Fe_{1.4}$	1.174	1.564	0.751	2	1	15.660	1.078	223.38	29.19
25	$LaNi_{4.7}Al_{0.3}$	$CeNi_3Cu_2$	1.039	1.452	0.716	0.444	1	51.122	15.518	183.89	46.57
26	$LaNi_{4.81}Mn_{0.28}Al_{0.15}$	$Ce_{1.1}Ni_{2.6}Cu_{2.6}$	1.003	1.546	0.649	0.234	1	35.947	7.232	196.62	46.94
27	$LaNi_{4.64}Mn_{0.36}$	$CeNi_{2.6}Cu_{2.6}$	0.997	1.447	0.689	0.538	1	56.178	9.641	204.62	25.59
28	$LaNi_{4.56}Mn_{0.44}$	$Ce_{1.1}Ni_{2.6}Cu_{2.6}$	0.972	1.524	0.638	0.313	1	35.947	6.342	199.60	41.62

Applicable MH alloy pairs for T_m=140 ℃

Pair no	MH alloy pair		COA	COAc	ψ	W_1	W_2	P_h	P_l	T_h	T_l
	HT MH alloy	LT MH alloy	–	–	–	kg	kg	bar	bar	°C	°C
1	$LaNi_{4.65}Mn_{0.35}$	$CeNi_3Cu_2$	0.954	1.405	0.679	0.54	1	57.100	12.669	205.44	35.69
2	$LaNi_{4.6}Al_{0.4}$	$CeNi_3Cu_2$	0.956	1.421	0.673	0.59	1	57.100	12.816	207.81	36.29
3	$LaNi_{4.65}Mn_{0.35}$	$CeNi_{2.5}Cu_{2.5}$	1.026	1.447	0.709	0.538	1	63.472	12.669	210.83	38.08
4	$LaNi_{4.6}Al_{0.4}$	$CeNi_{2.5}Cu_{2.5}$	1.030	1.464	0.703	0.589	1	63.472	12.816	213.47	38.63
5	$LaNi_{4.25}Al_{0.75}$	$Zr_{0.9}Ti_{0.1}Cr_{0.6}Fe_{1.4}$	1.139	1.532	0.743	1.96	1	29.740	3.644	220.22	43.32
6	$LaNi_{4.83}Mn_{0.17}$	$CeNi_4Cr$	1.310	1.482	0.884	3.35	1	146.246	28.372	220.57	35.47
7	$LaNi_{4.8}Al_{0.2}$	$CeNi_4Cr$	1.288	1.477	0.873	4.95	1	146.246	30.032	216.25	38.20
8	$LaNi_{4.83}Mn_{0.17}$	$CeNi_3Cr_2$	1.260	1.422	0.887	3.65	1	125.899	28.372	211.93	32.49
9	$LaNi_{4.8}Al_{0.2}$	$CeNi_3Cr_2$	1.245	1.417	0.879	5.41	1	125.899	30.032	207.85	35.55
10	$LaNi_{4.75}Al_{0.25}$	$CeNi_3Cr_2$	1.240	1.419	0.874	4.62	1	125.899	24.261	220.38	24.35
11	$Fe_{0.8}Ni_{0.2}Ti$	$CeNi_{2.5}Cu_{2.5}$	0.996	1.412	0.705	0.464	1	63.472	10.655	212.62	30.05
12	$Fe_{0.8}Ni_{0.2}Ti$	$CeNi_3Cu_2$	0.922	1.373	0.672	0.465	1	57.100	10.655	207.61	26.98

$$Q_h = n_{t1}\Delta H_1 + (n_1 Cv_1 + W_{1R}Cp_{1R})(T_h - T_m)$$

$$Q_{m1} = n_{t2}\Delta H_1 + (n_1 Cv_1 + W_{1R}Cp_{1R})(T_h - T_m)$$

$$Q_{m2} = n_{t1}\Delta H_2 - (n_2 Cv_2 + W_{2R}Cp_{2R})(T_m - T_l)$$

$$Q_l = n_{t2}\Delta H_2 - (n_2 Cv_2 + W_{2R}Cp_{2R})(T_m - T_l)$$

$$COA = \frac{Q_{m1}+Q_{m2}}{Q_h}$$

$$COA_c = \frac{T_m(T_h-T_m)}{T_h(T_m-T_l)}$$

$$\psi = \frac{COA}{COA_C}$$

MH Alloy for MH1 (HT): $LaNi_{4.25}Al_{0.75}$
MH Alloy for MH2(LT): $Zr_{0.9}Ti_{0.1}Cr_{0.6}Fe_{1.4}$

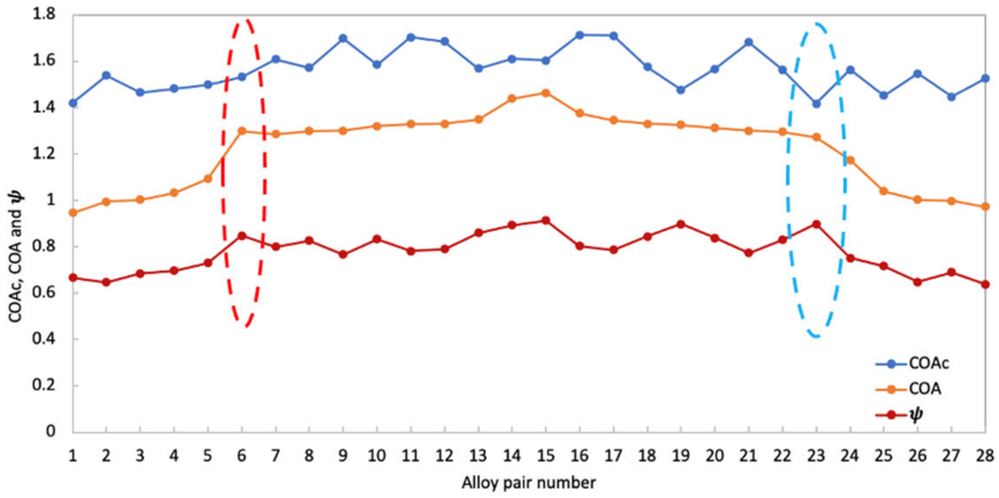

Variation of COA, COA_c and ψ with different alloy pair numbers for T_m=130 °C

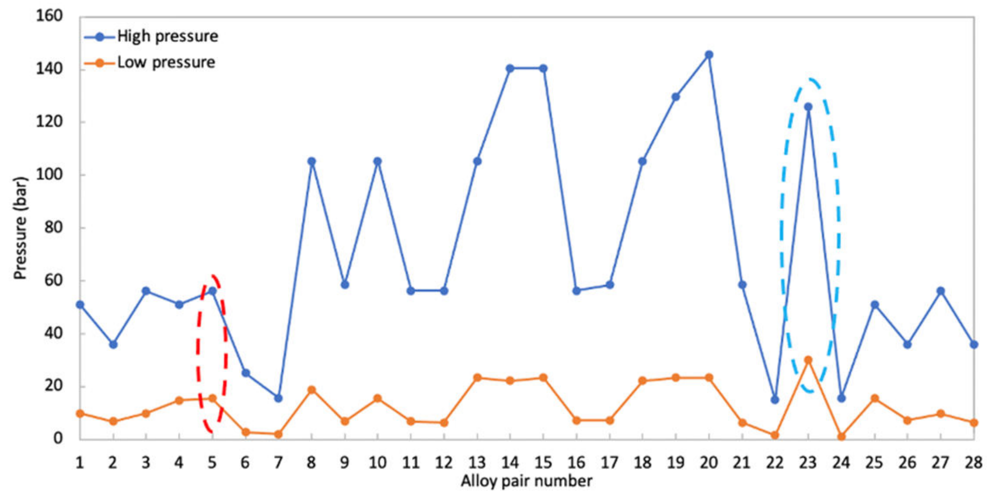

Variation of high and low hydrogen pressures with different alloy pair numbers for T_m=130 °C

PCT Phase diagrams with correlations and measurements

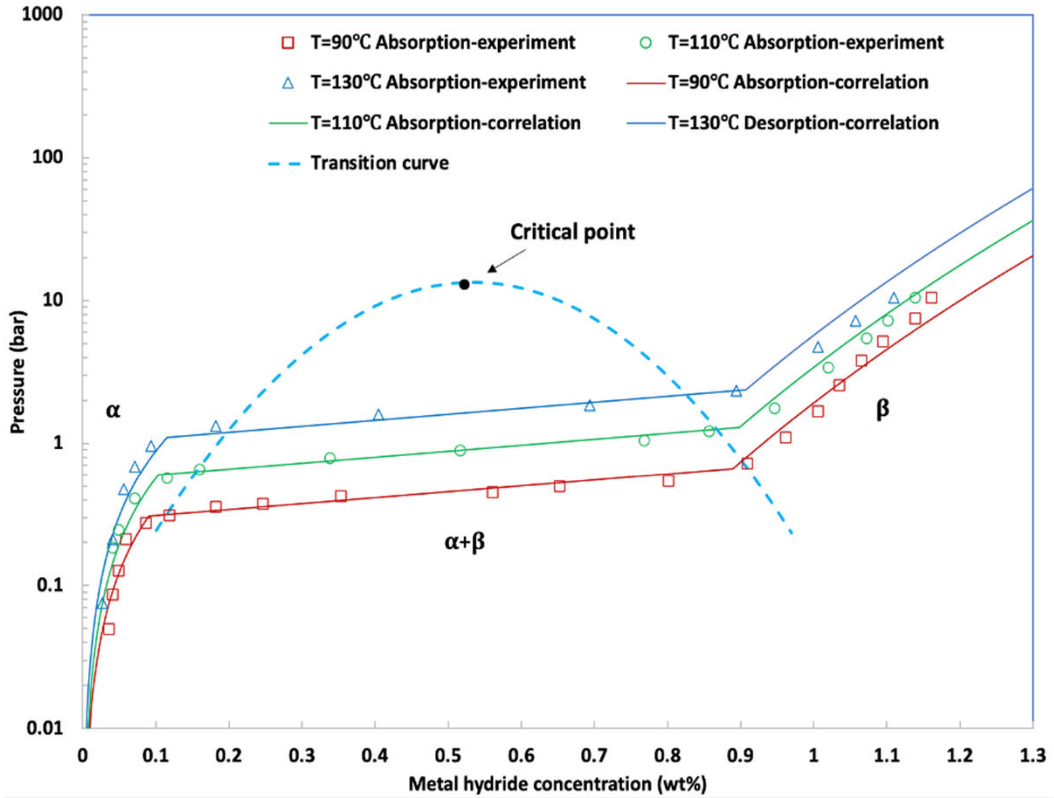

Figure 6 PCT phase diagram with correlations of three regions using limited measurement data for MH alloy **$LaNi_{4.25}Al_{0.75}$ isothermal absorption**

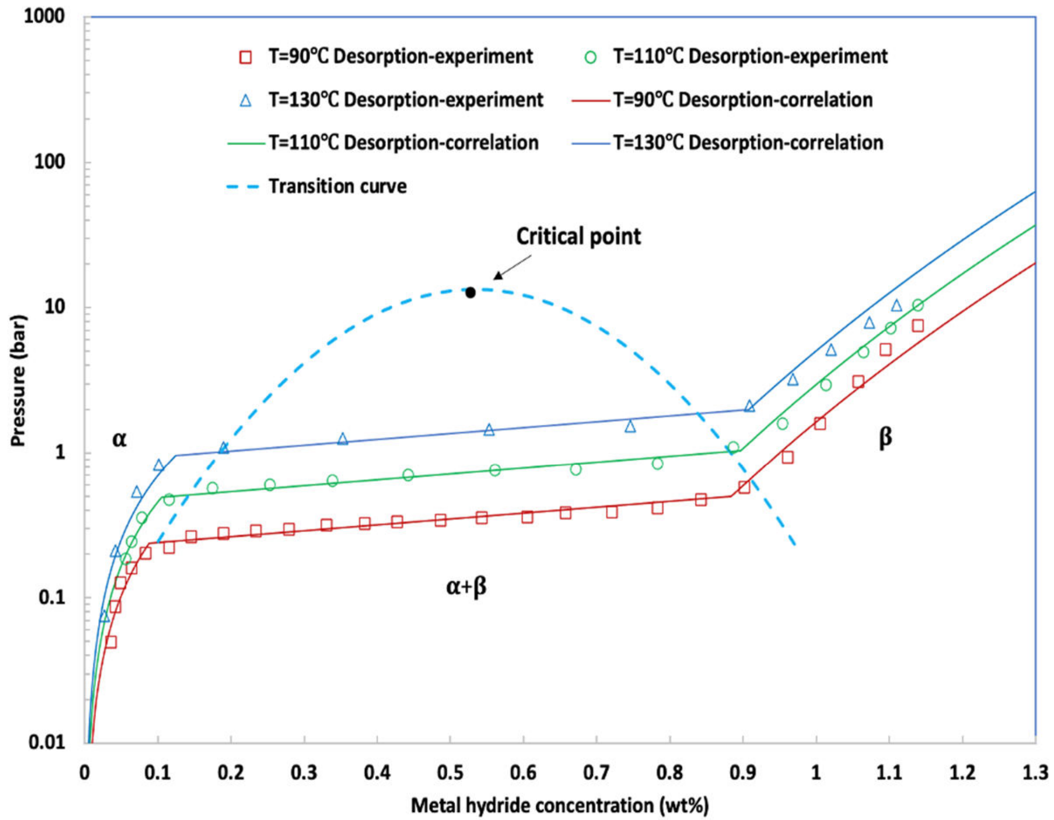

Figure 7 PCT phase diagram with correlations of three regions using limited measurement data for MH alloy **$LaNi_{4.25}Al_{0.75}$ isothermal desorption**

Engineering and Physical Sciences Research Council

London South Bank University

Innovate UK

Average relative errors between correlations and measurement data

MH Alloy	α region		α+β region		β region	
	Absorption %	Desorption %	Absorption %	Desorption %	Absorption %	Desorption %
$LmNi_{4.91}Sn_{0.15}$	10.35	18.38	4.03	6.47	1.49	2.13
$Ti_{0.99}Zr_{0.01}V_{0.43}Fe_{0.09}Cr_{0.05}Mn_{1.5}$	20.99	9.32	9.89	1.95	2.20	1.28
$LaNi_{4.25}Al_{0.75}$	13.79	9.68	9.54	5.90	1.99	1.31
$Zr_{0.9}Ti_{0.1}Cr_{0.6}Fe_{1.4}$	10.25	10.61	2.40	4.92	2.27	1.43

Engineering and Physical Sciences Research Council
London South Bank University
Innovate UK

Test rig development of MH heat pump system

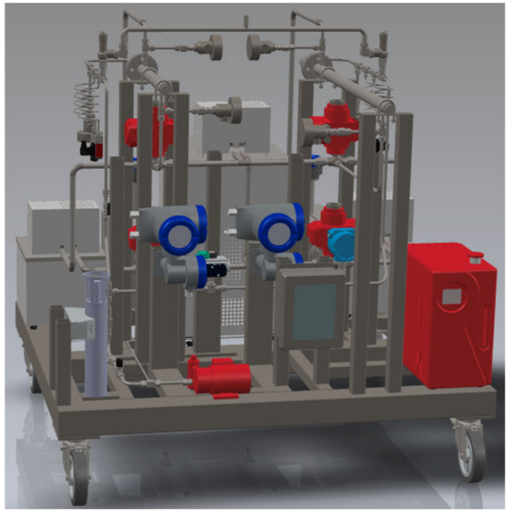

Test rig of MHHP

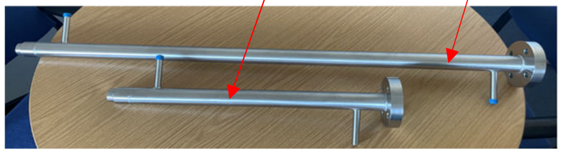

Two MH reactors (MH1 and MH2) in the rig

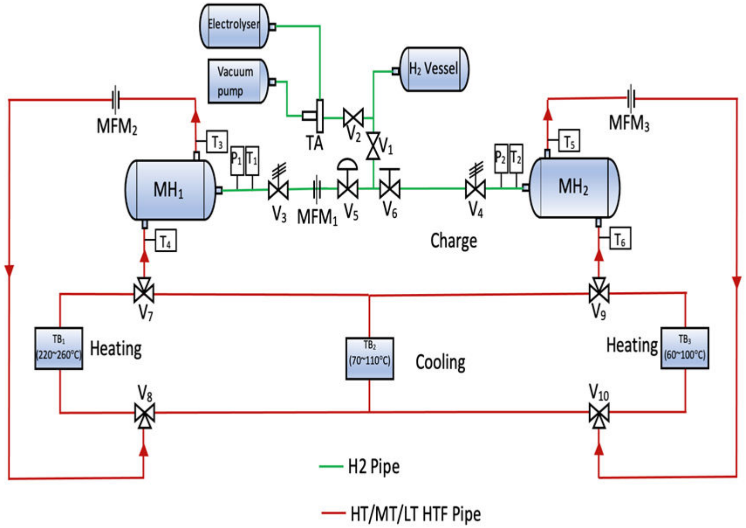

Test rig layout

UKRI Engineering and Physical Sciences Research Council

London South Bank University EST 1892

UKRI Innovate UK

Description of operation cycle

Low-pressure operation c→d

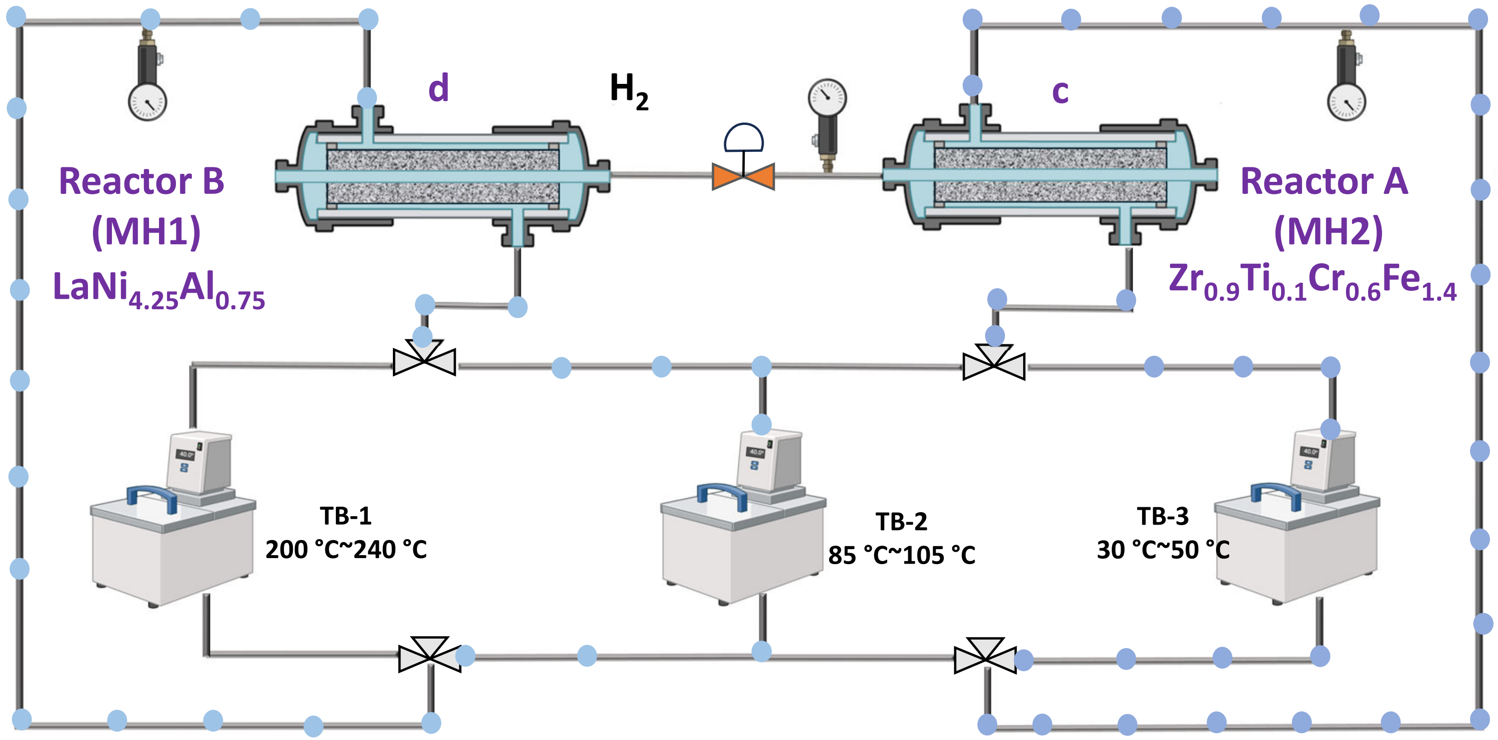

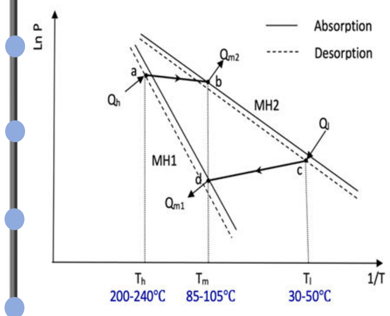

Engineering and Physical Sciences Research Council

London South Bank University

Innovate UK

Description of operation cycle

High-pressure operation a→b

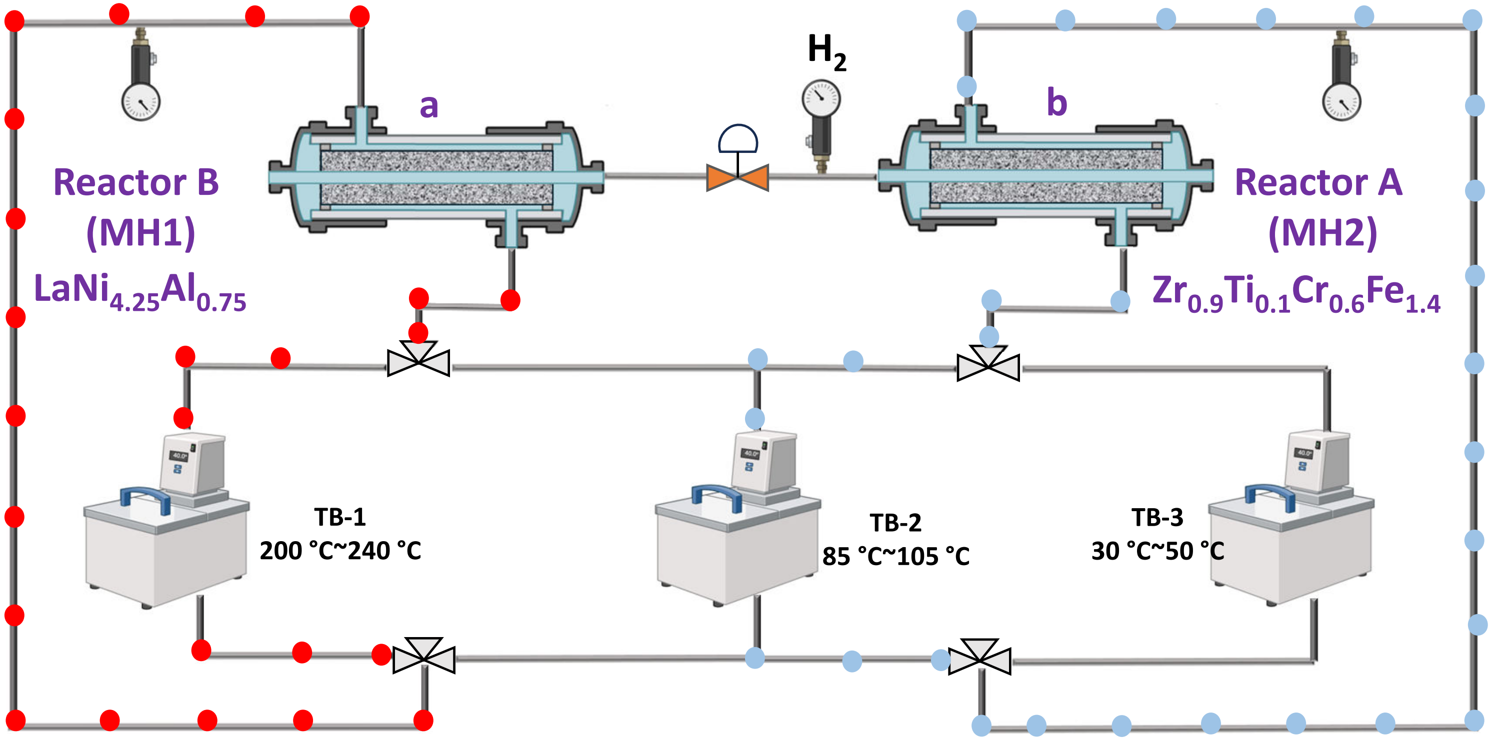

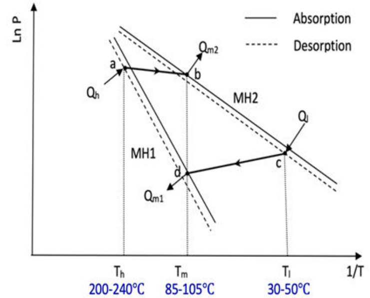

Engineering and Physical Sciences Research Council

London South Bank University

Innovate UK

Test rig is allocated in a purposely built hydrogen lab

Engineering and Physical Sciences Research Council

London South Bank University
EST 1892

Innovate UK

CFD model

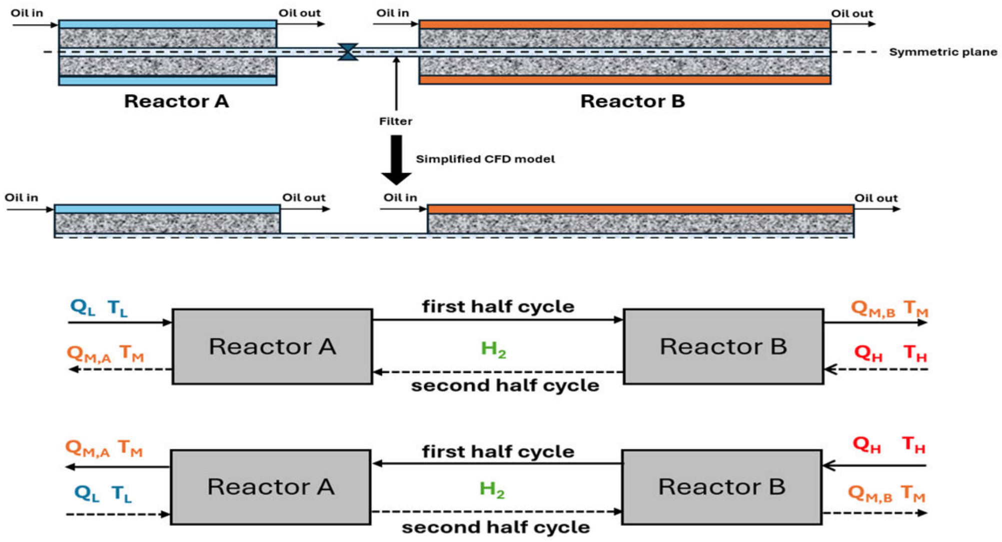

(a)

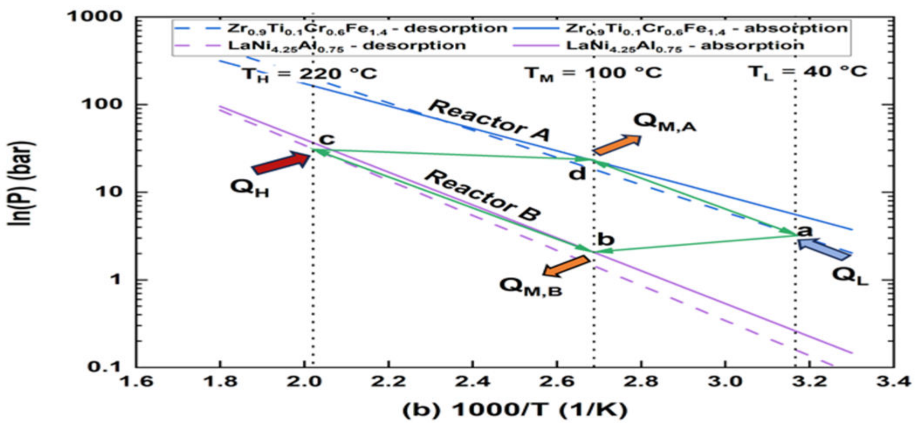

Schematic of the coupled reactor and its operating cycle on a Van't Hoff plot

Two purposely designed metal hydride reactors in a MHHP system

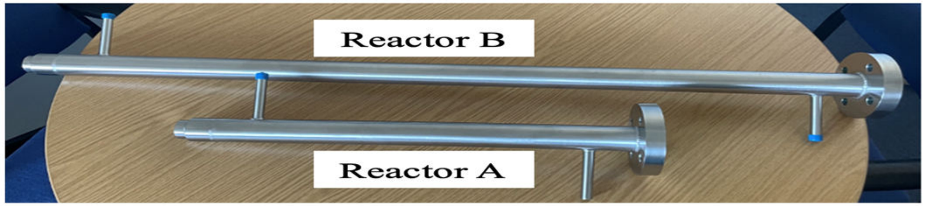

Design data for each MH reactor and connection pipe

Reactor	Do_{fi} (mm)	Di_{fi} (mm)	Do_{mh} (mm)	Di_{mh} (mm)	Do_{re} (mm)	Di_{re} (mm)	Do_{cn} (mm)	Di_{cn} (mm)
MH1	12.7	9.52	33.4	27.86	42.16	36.62	12.7	9.52
MH2	12.7	9.52	33.4	27.86	42.16	36.62	12.7	9.52

Model Equations

Mass equation:

$$(1-\mathcal{E})\frac{\partial \rho_m}{\partial t} = \dot{m}$$

Energy equation:

$$(\rho C_p)_e \frac{\partial T_m}{\partial t} + \rho_g C_p^g \vec{V}_g \nabla T_m = \nabla(K_e \nabla T_m) + \dot{m}[\Delta H + T_m(C_p^g - C_p^m)]$$

Effective thermal conductivity:

$$K_{eff} = \mathcal{E}K_g + (1-\mathcal{E})K_m$$

Absorption reaction kinetic equation:

$$\dot{m}_a = C_a \exp\left(-\frac{E_a}{RT}\right) \ln\left(\frac{P_g}{P_{eq}}\right)(\rho_{sat} - \rho_s)$$

Desorption reaction kinetic equation:

$$\dot{m}_d = C_d \exp\left(-\frac{E_d}{RT}\right)\left(\frac{P_{eq}-P_g}{P_{eq}}\right)(\rho_{sat} - \rho_s)$$

Van't Hoff equation:

$$lnP_{eq} = -\frac{\Delta H}{RT} + \frac{\Delta S}{R} + f_S(C - C_{max}/2)$$

CFD model

Performance parameters

The Coefficient of Performance (COP) of a metal hydride heat pump :

$$COP = \frac{Q_{M,A}+Q_{M,B}}{Q_H}$$

Where Q_H represents the high-grade useful heat input obtained at the heat input temperature, T_H. Q_M denotes the heat output at T_M.

$$Q_H = n\Delta H_{B,d} + \dot{m}_B Cp_B(T_H - T_M)$$

$$Q_{M,A} = n\Delta H_{A,a} - \dot{m}_A Cp_A(T_M - T_L)$$

$$Q_{M,B} = n\Delta H_{B,a} + \dot{m}_B Cp_B(T_H - T_M)$$

The average heat transfer rate for each process over the time period from the starting time t_1 to the end time t_2, with a duration of ΔT can be calculated as follows:

$$\overline{Q} = \frac{\int_{t1}^{t2} Q dt}{\Delta T}$$

The specific heat power defined as the cumulative heat output obtained over a complete cycle per unit mass of alloy:

$$SHP = \frac{Q_m}{(m_A+m_B)t_{cycle}}$$

Engineering and Physical Sciences Research Council

London South Bank University

Innovate UK

model validations

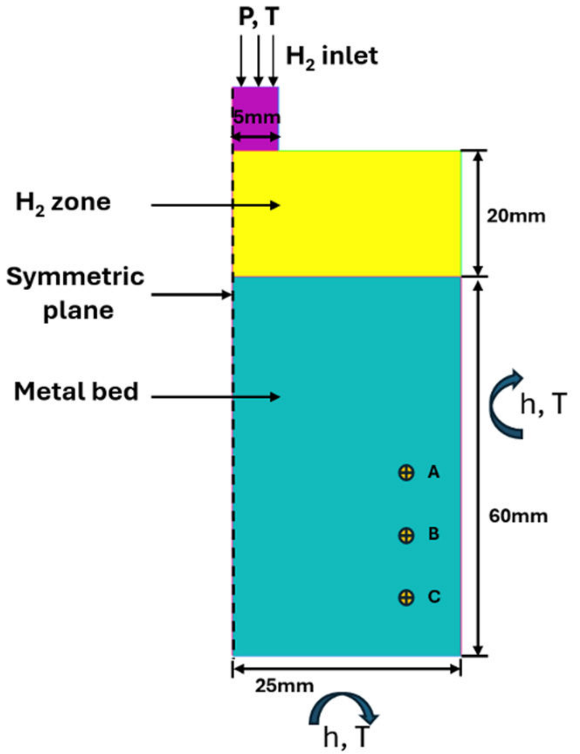

Fig.2. Geometry of validated reactor.

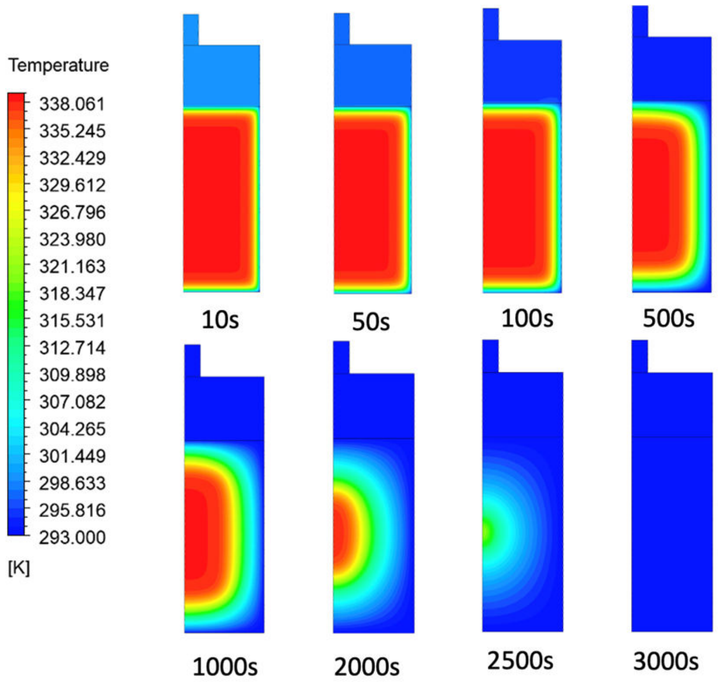

Fig.3. Temperature distributions during absorption.

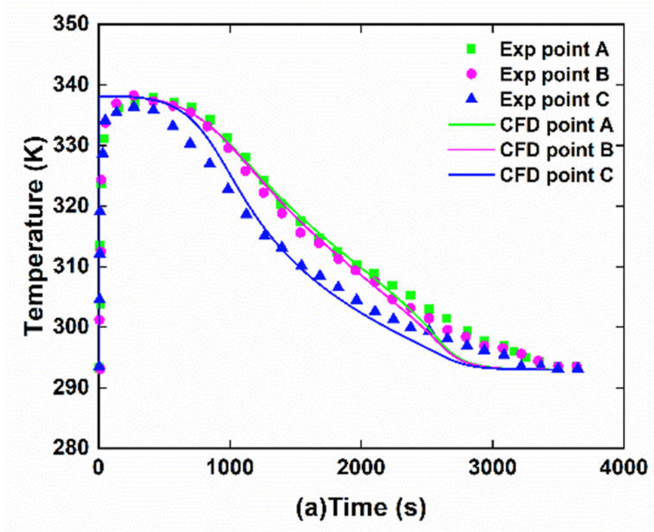

Absorption

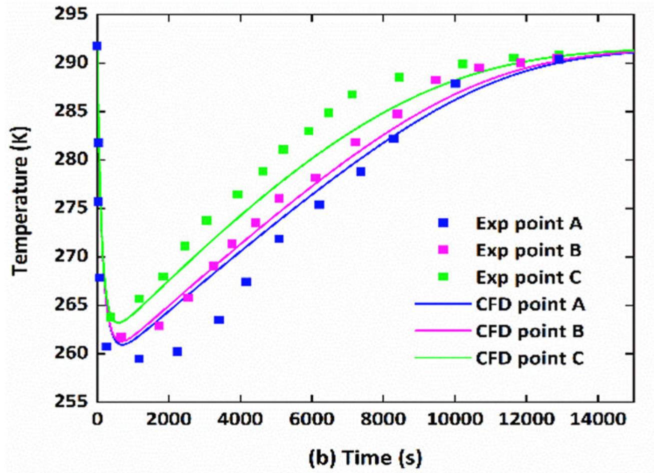

Desorption

Engineering and Physical Sciences Research Council

London South Bank University

Innovate UK

CFD Model Validation

Design and operating data and properties

Metal hydride alloy	Process	ΔH	ΔS	C_{max}	f_S	E	C_a/C_d	C_p^m	C_p^g	k_{eff}	ε	ρ
$Zr_{0.9}Ti_{0.1}Cr_{0.6}Fe_{1.4}$	Absorption	24500 [20]	92 [20]	1.47% [30]	0.216 [31]	26000 [20]	265 [20]	419	14890	4.028	0.507	8400 [20]
	Desorption	29770 [20]	104.13 [20]		0.251 [31]	23500 [20]	45 [20]					
$LaNi_{4.25}Al_{0.75}$	Absorption	35900 [32]	102.5 [32]	1.13% [33]	0.963 [31]	24065 [34]	57 [35]			2.944	0.645	7600 [33]
	Desorption	38300 [32]	106 [32]		0.94 [31]	19430 [34]	9.57 [35]					

Designed operating condition	
High-grade heat source temperature (T_H)	493 [K]
Medium heat sink temperature (T_M)	373 [K]
Low-grade heat source temperature (T_L)	313 [K]
HTF mass flow rate	0.14 [kg s^{-1}] ($u = 0.9$ m/s)

Temperature distributions

Reactor A **Reactor B**

Refrigeration (a-b)

Sensible heating b-c and a-d

Regeneration c-d

Sensible cooling c-b and d-a

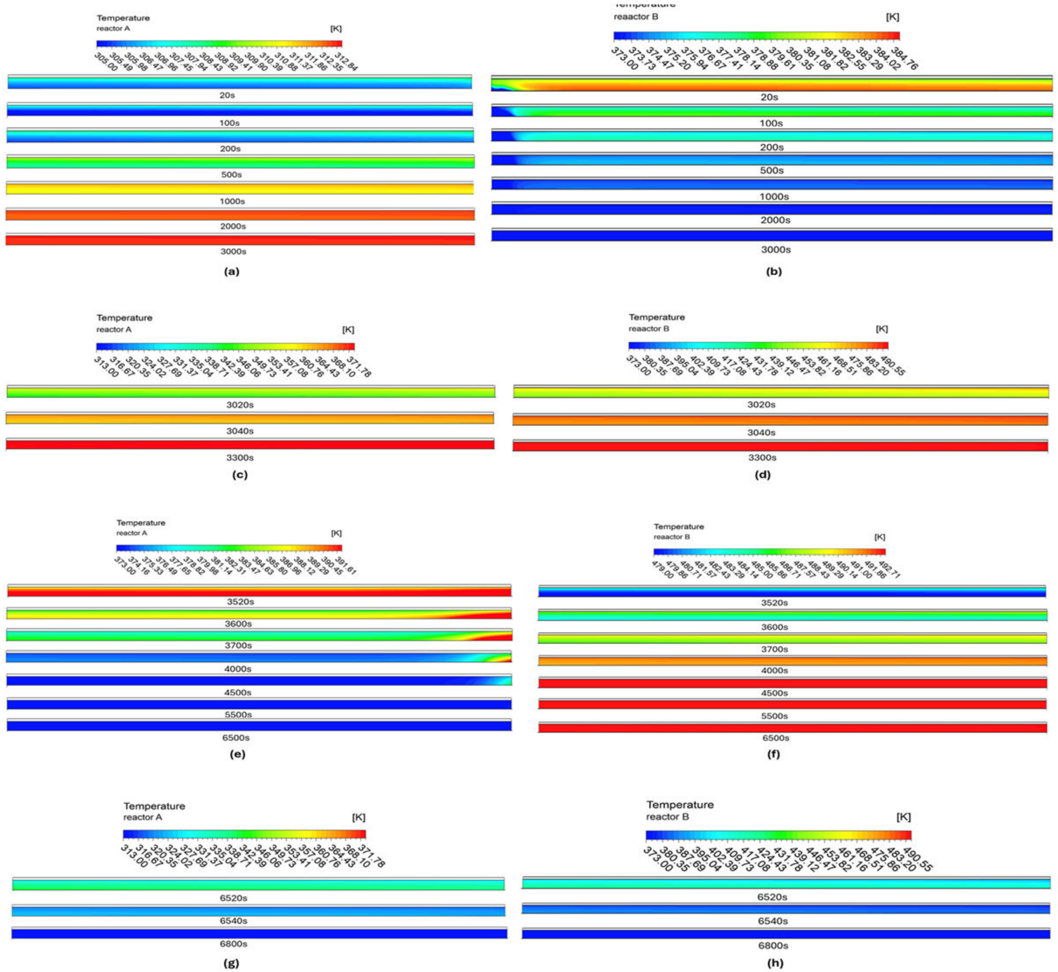

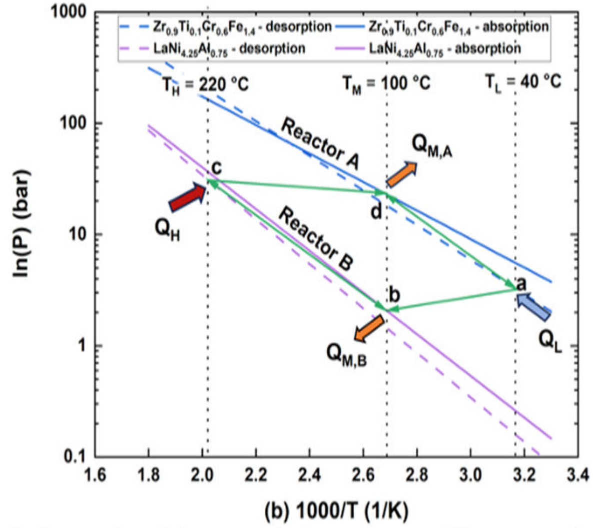

Dynamic parameter variations

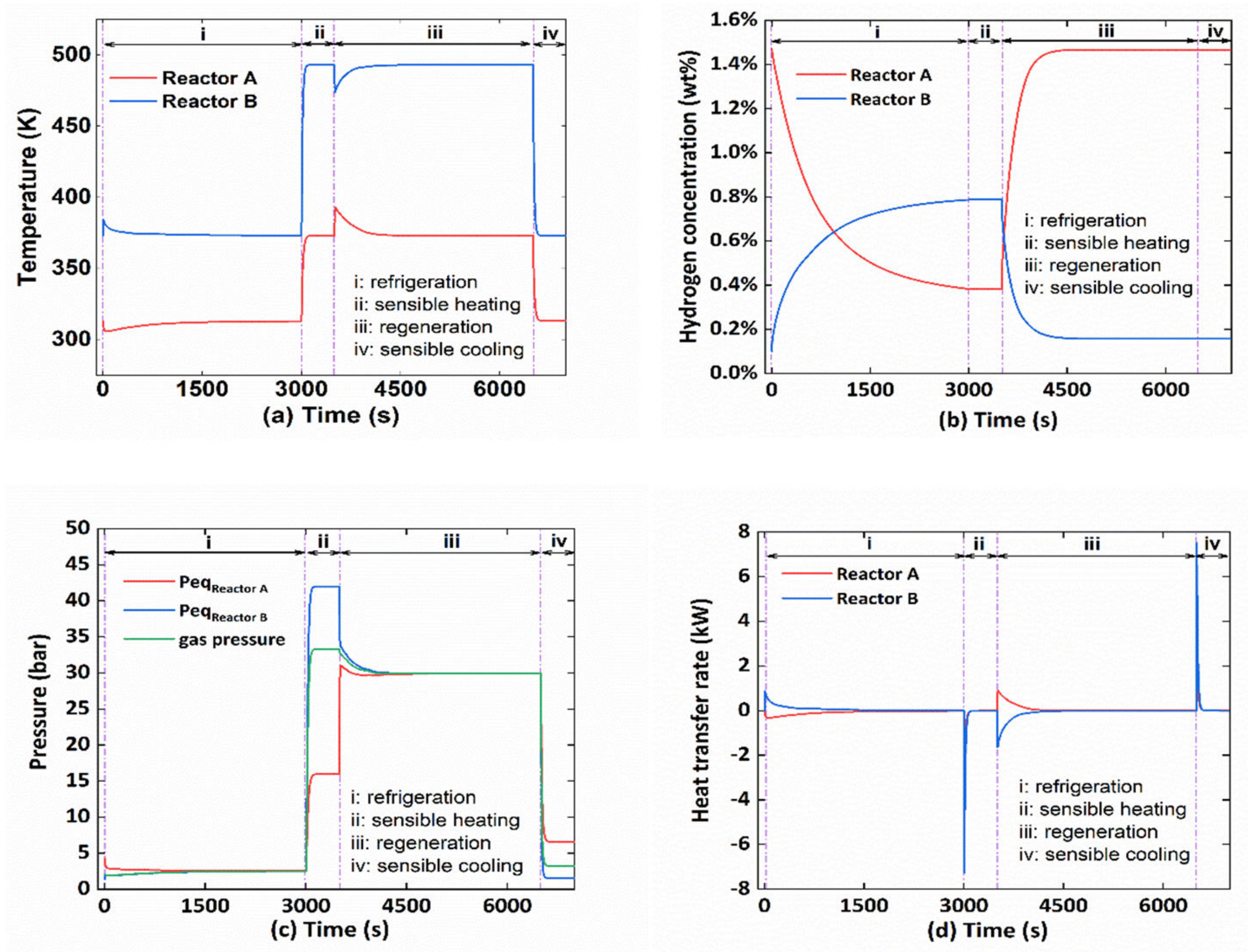

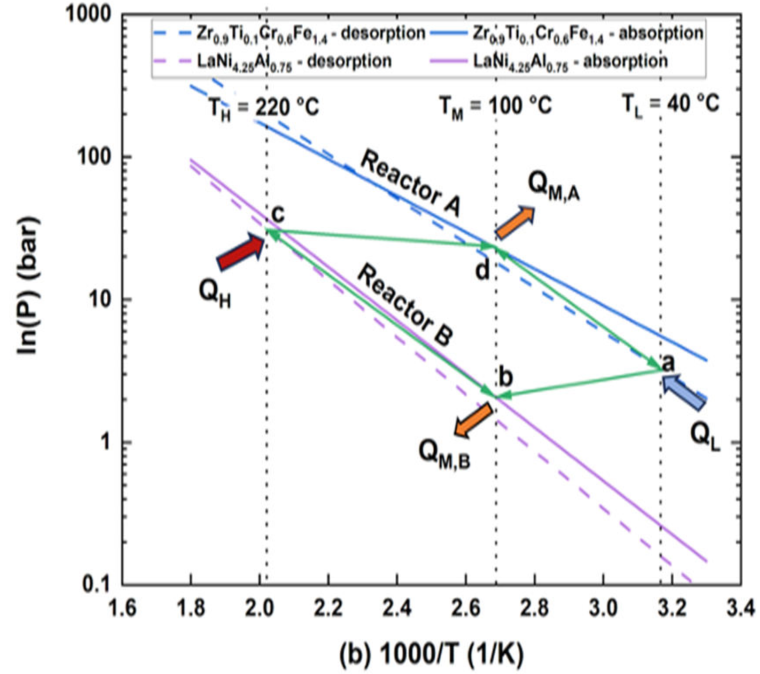

Engineering and Physical Sciences Research Council

London South Bank University

Innovate UK

Performance evaluation at different operating conditions

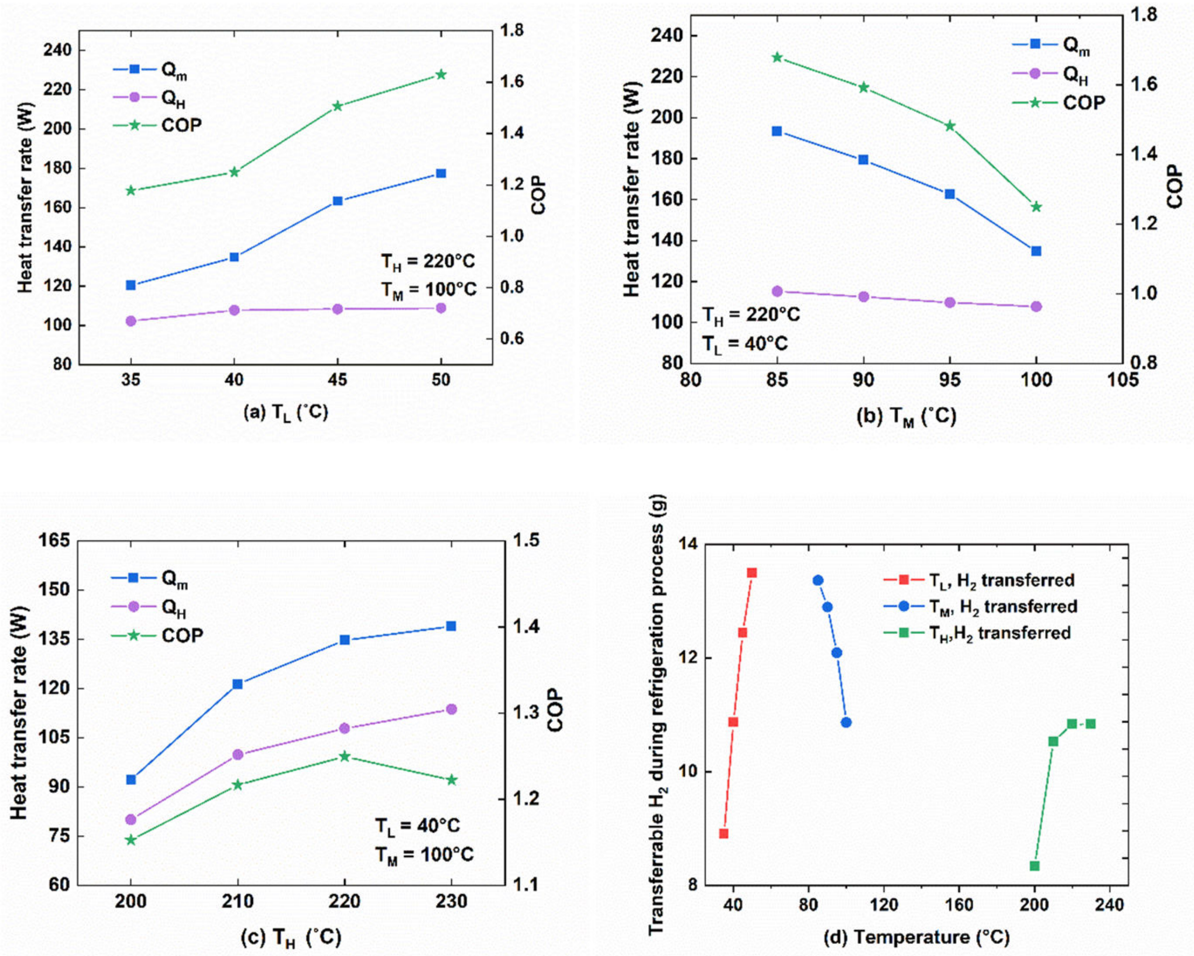

$$SHP = \frac{Q_m}{(m_A + m_B)t_{cycle}}$$

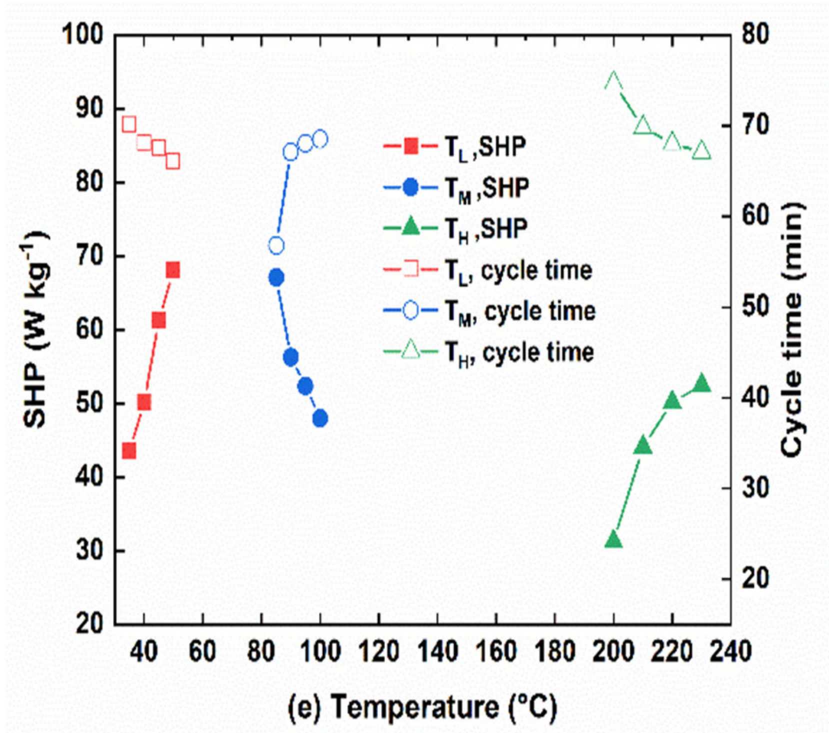

Engineering and Physical Sciences Research Council

London South Bank University

Innovate UK

Effects of thermal conductivity

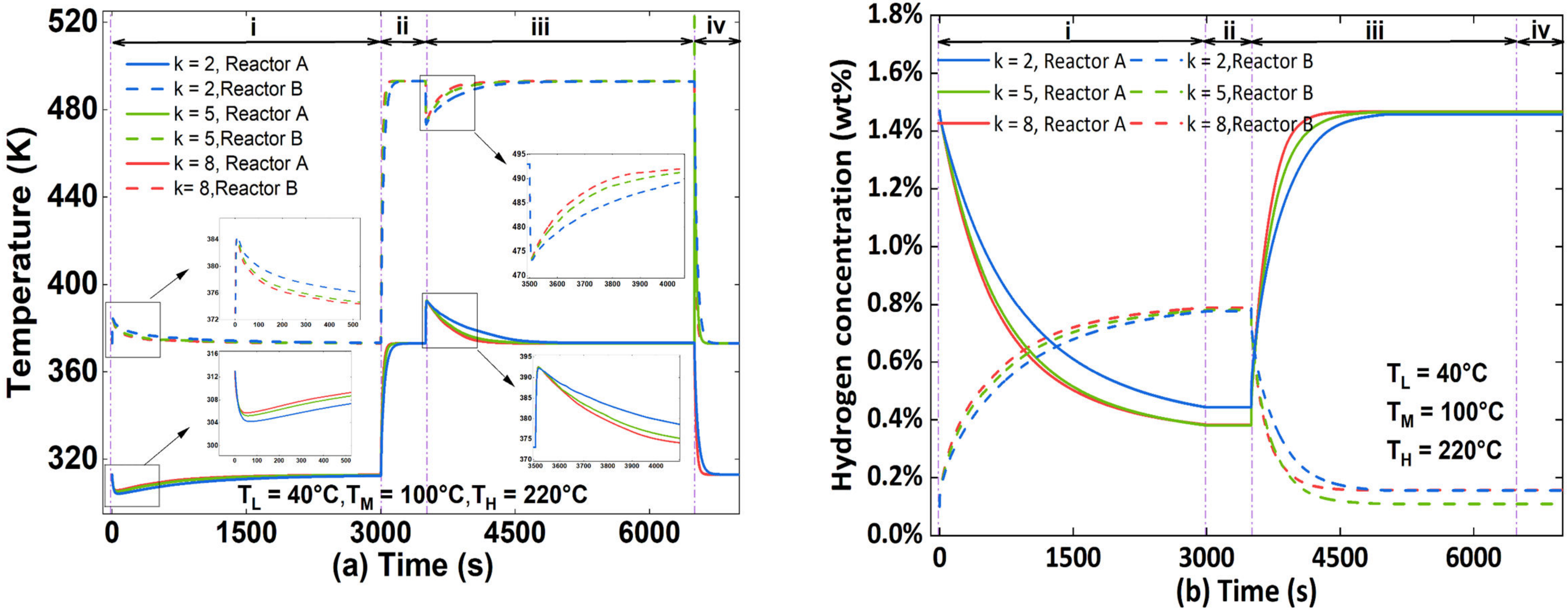

Effects of thermal conductivity on average volume temperature and hydrogen concentration of metal hydride bed

Effects of thermal conductivity

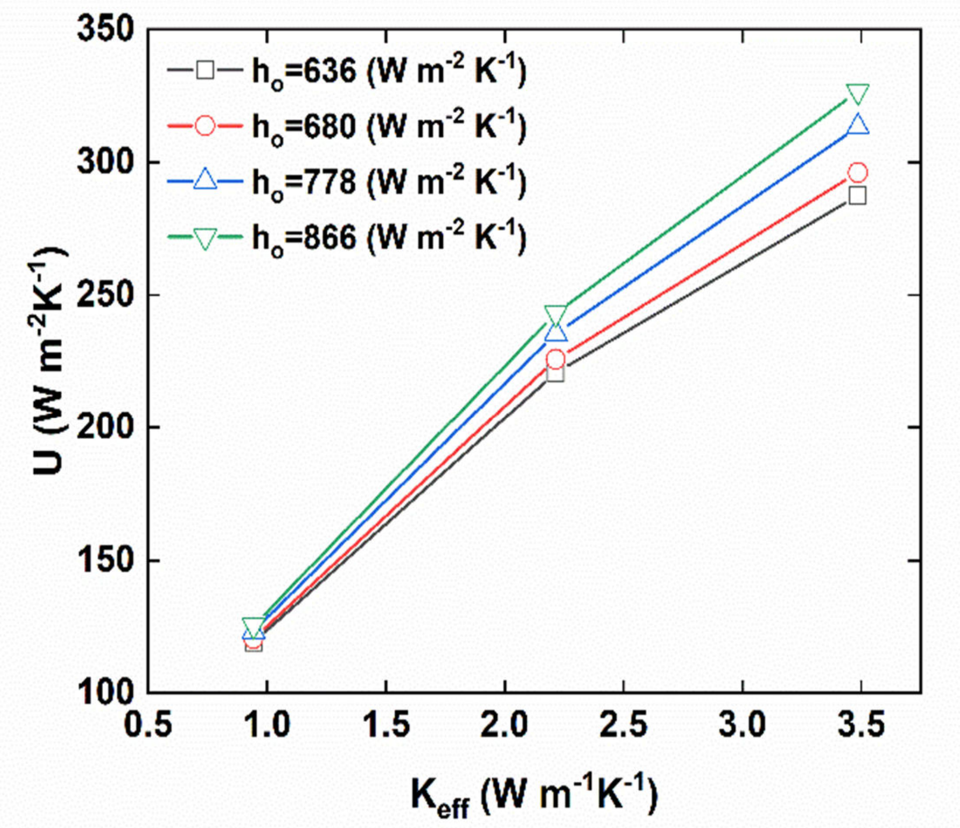

Effects of effective thermal conductivity on the overall heat transfer

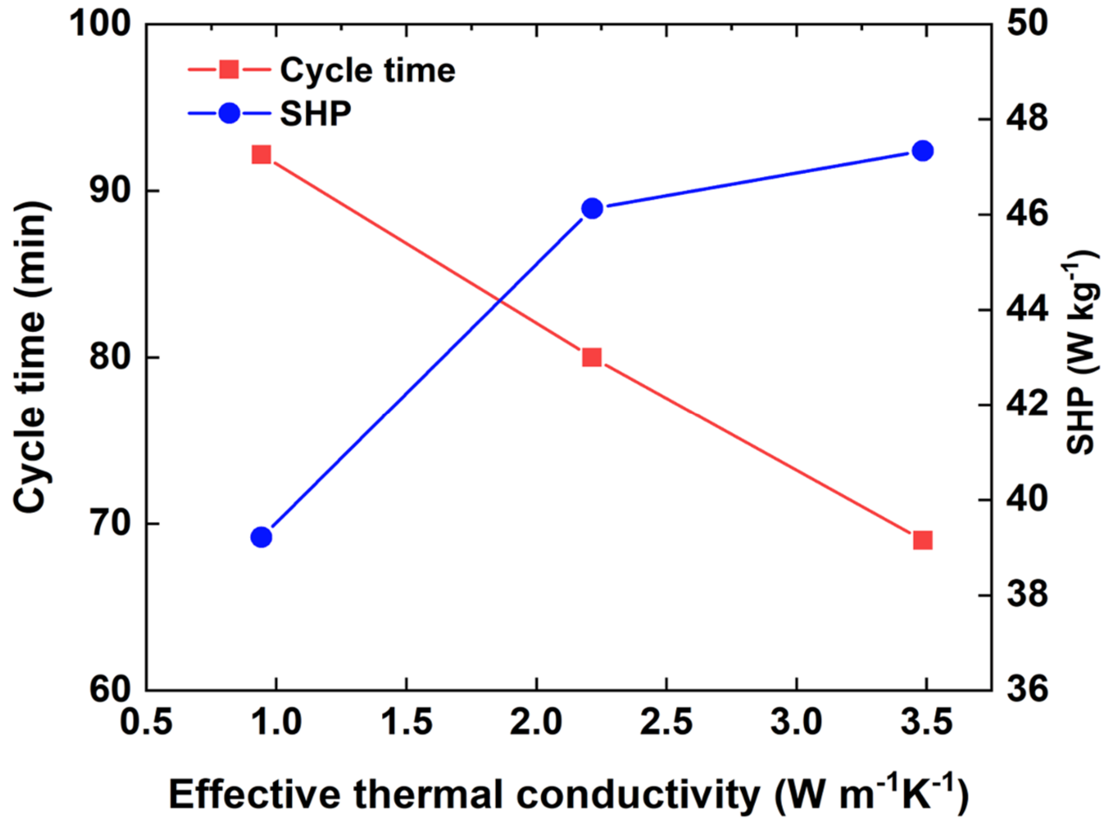

Effects of thermal conductivity on cycle time and SHP

Engineering and Physical Sciences Research Council

London South Bank University

Innovate UK

Conclusions

- One metal hydride pair has been identified for the high-temperature MH heat pump;
- Correlation models of PCT phase diagram have been developed to characterize any MH alloy based on limited measurement data;
- A transient model of the MH heat pump system has been developed;
- The model can be used for the optimisation of system design and operation.

Engineering and Physical Sciences Research Council
London South Bank University
Innovate UK

Thanks